P H Y S I C A L   R E V I E W   L E T T E R S

Saturated Ionization of Fullerenes in Intense Laser Fields

A. Jaroń-Becker,[1,2] A. Becker,[2] and F. H. M. Faisal[3]

[1]*Institut für Physikalische Chemie und Elektrochemie, Technische Universität Dresden, D-01062 Dresden, Germany*
[2]*Max-Planck-Institut für Physik komplexer Systeme, Nöthnitzer Strasse 38, D-01187 Dresden, Germany*
[3]*Fakultät für Physik, Universität Bielefeld, Postfach 100131, D-33501 Bielefeld, Germany*
(Received 31 January 2006; published 14 April 2006)

We investigate the ionization of icosahedral fullerenes (C_{20}, C_{60}, C_{80}, and C_{180}) in an intense laser pulse using the *S*-matrix theory. The results obtained are in excellent agreement with the recent observations of unexpectedly high saturation intensities of the Buckminster fullerene and its multiply charged ions. Our analysis strongly suggests that the related phenomenon of suppressed ionization of these complex fullerenes is due to the finite cage size and the "multislit" interference effect between partial waves emitted from the different nuclei rather than to a dynamical multielectron polarization effect.

The response of many-body electronic systems, such as complex atoms, molecules, and clusters, with intense femtosecond light pulses is one of the most vigorously pursued research topics in nonperturbative light-matter interaction physics. Currently available laser intensities can be made so high as to saturate the probabilities of ionization to higher charge states of the initially neutral many-electron targets. One of the basic questions regarding such interactions is whether the response is dominated by dynamical one-electron or multielectron mechanisms. A second, related problem is the origin of the systematically higher ionization saturation intensities observed for complex multielectron multicenter molecules than that of the so-called "companion atoms" having equal ionization energies and a point center [1–3]. In this Letter, we consider both the problems by analyzing the recently observed saturation intensities of the fullerene molecule C_{60} and its multiply charged ions [3] as well as of other icosahedral fullerenes up to C_{180}.

The fundamental interaction of photons with a many-electron system is given by the independent sum of *one-body* interactions [e.g., in dipole length gauge $V(t) = \sum_{i=1}^{N_e} \boldsymbol{E}(t) \cdot \boldsymbol{r}_i$, where $\boldsymbol{E}(t)$ is the electric field and N_e is the number of electrons, e.g., in the valence shell of the atom or molecule]. This simple fact lies essentially behind the dynamical one-electron response of atomic and simple molecular systems in single ionization processes. It has been often confirmed by *ab initio* numerical simulations (e.g., [4,5]), Floquet calculations (e.g., [6,7]), and by calculations using the tunneling (e.g., [8–11]) or the Keldysh-Faisal-Reiss (KFR) models [8,12,13], as well as the related *S*-matrix theories (e.g., review [14]).

However, recent experiments on ionization of C_{60} have revealed unexpectedly high saturation intensities for the fullerene and its multiply charged ions [3]. This has been interpreted [3,15,16] to have shown that the hypothesis of a one-electron response fails for large molecules (C_{60} being a prototype of it) and to arise from a multielectron polarization effect. Below, we show instead that the ex-

perimental data can be well understood to be due to the finite cage size and multislit interference effects between partial waves emitted from the different nuclei of the fullerene.

For the analysis, we have used the lowest-order *S*-matrix theory, known usually as KFR theory [8,12,13]. The calculations take account of the icosahedral structural symmetry, the finite size of the atomic "cage," and the multicenter nuclear positions of the fullerenes. Thus, we represent the molecular orbitals of the fullerenes and their ions as a linear combination of atomic orbitals $\phi_{i,j}$, centered at the nuclear positions $\boldsymbol{R}_i$, $i = 1, 2, \ldots n$ (Hartree atomic units $e = m = \hbar = 1$ are used):

$$\phi_i(\boldsymbol{r}, \boldsymbol{R}_1, \ldots, \boldsymbol{R}_n) = \sum_{i=1}^{n} \sum_{j=1}^{j_{\max}} a_{i,j} \phi_{i,j}(\boldsymbol{r}, \boldsymbol{R}_i), \qquad (1)$$

where n is the total number of nuclei in the molecule, $a_{i,j}$ are the variational coefficients of the atomic basis functions, and $j_{\max}$ is the size of the basis set used. The orbitals are obtained by locating the equivalent carbon atoms at positions $\boldsymbol{R}_i$ according to the icosahedral symmetry of the fullerene and using the self-consistent Hartree-Fock method with Gaussian basis functions [17].

The lowest-order *S*-matrix ionization amplitude is given by the transition matrix element between the initial molecular state and the emitted electron in the dressed Volkov state. Using the velocity gauge, performing the spatial and time integration analytically, and modulo squaring the resulting expression, we obtain the basic *rate* of ionization as an analytical formula:

$$\Gamma^+(I) = 2\pi N_e C^2(Z, E_B, F) \sum_{N=N_0}^{\infty} \int d\hat{\boldsymbol{k}}_N k_N (U_p - N\omega)^2$$

$$\times J_N^2\left(\boldsymbol{\alpha}_0 \cdot \boldsymbol{k}_N, \frac{U_p}{2\omega}\right) \left| \sum_{i=1}^{n} M_i(\mathbf{k}_N; \boldsymbol{R}_i) \right|^2, \qquad (2)$$

where

$$M_i(\mathbf{k}_N; \boldsymbol{R}_i) = \sum_{j=1}^{j_{max}} a_{i,j} \langle \phi_0(\mathbf{k}_N, r) | \phi_{i,j}(r, \boldsymbol{R}_i) \rangle \qquad (3)$$

is the partial amplitude of the bound-free matrix element (or Fourier transform) of the molecular orbital at the ith nuclear center. In the above, the angle brackets denote the spatial volume integration. N_e is the number of equivalent electrons in the highest occupied molecular orbital (HOMO) of the target molecule, E_B is the ionization potential of the molecule, and $U_p = I/4\omega^2$ is the ponderomotive potential. $k_N = \sqrt{2(N\omega - E_B - U_p)}$ is the momentum of the Volkov electron on absorbing N photons, and $\phi_0(\mathbf{k}_N, r)$ is the plane wave of momentum k_N. $J_n(a; b)$ is the generalized Bessel function of two arguments; $\alpha_0 = \sqrt{I}/\omega^2$ is the "quiver radius" of oscillation of a free electron along the direction of a linearly polarized laser field (here chosen as the z direction) of peak intensity I and frequency ω.

Note the presence of the factor C^2 in Eq. (2), which arises from the Coulomb correction of the plane-wave Volkov wave function. In the atomic case [18,19], it is given by $C^2_{atom} = (4E_B/Fr_{atom})^{2Z/k_B}$, where $r_{atom} \equiv 2/k_B$, with $k_B \equiv \sqrt{2E_B}$ the radius of the turning point of the atomic electron in the bound state and F the field strength. This Coulomb correction yields good agreement with the calculations of *ab initio* simulations and Floquet calculations as well as with a large set of experimental data for the ionization rates and yields of atoms [19]. In the present case of the fullerenes, therefore, we have employed an analogous Coulomb correction, where the radius r_{atom} is simply extended to $R + \delta a$, where R is the hard-sphere radius of the cage and $\delta a (\approx 2/k_B)$ is the spill-out radius of the electron cloud (e.g., [20]). This gives for the fullerenes

$$C^2(Z, E_B, F) = \left(\frac{4E_B}{F(R + \delta a)} \right)^{2Z/\sqrt{2E_B}}. \qquad (4)$$

In order to compare the theoretical results with the experimental data, we have determined the ion yield distributions by inserting the calculated ionization rates using Eq. (2) into the rate equations governing the populations (e.g., [21]), integrating them over the pulse profile, and adding the contributions from all the points in the Gaussian laser focus. The experimental saturation intensities have been extracted from the ion yields by extrapolating the high intensity linear part of the yields to the intensity axis and taking the intensity at the intersection point [2,3]. We have used the same procedure for defining the calculated saturation intensities. As can be seen from Fig. 1, there is excellent agreement between the theoretical and experimental results for the whole sequence of nine charge states of C_{60}^{Z+}, $Z = 1, 2, \ldots, 9$, that have been measured [3]. It is clear that the above result, as obtained from Eq. (2), is independent of dynamical many-electron effects and/or a polarization of the electron cloud, suggested earlier [3,16].
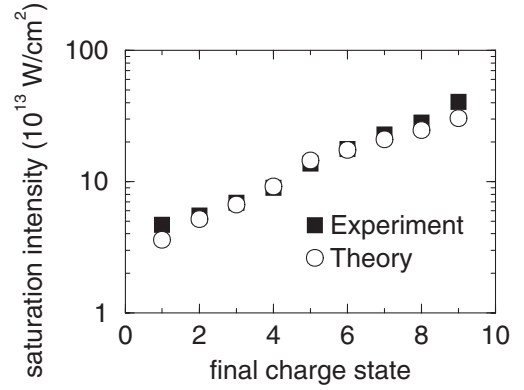

FIG. 1.   Comparison of the theoretical predictions for the saturation intensities for the first nine charge states of C_{60} (open circles) with the experimental data (solid squares, [3]) at a laser wavelength of 1500 nm and a pulse duration of 70 fs.

To investigate further the nature of the ionization process, we consider the saturation intensities as a function of wavelength. Figure 2 shows the calculated saturation intensities of C_{60}^+ over a wide range of wavelengths between 400 and 2200 nm. They increase at first with the increase of the wavelength until they reach a constant value at about 1000 nm and above. As in the well-known atomic case, this suggests a transition from the nonperturbative "multiphoton" to the "tunnel" regime, as characterized by the Keldysh parameter $\gamma = \sqrt{E_B/2U_p} > 1$ and $\gamma < 1$, respectively [8]. We may note that, in both the short and the long wavelength limits, the results agree well with the observations (400 nm [22,23] and 1200—2200 nm [3]).

Next, in Fig. 3(a), we show the calculated C_{60}^+ ion yields as a function of the peak intensity for the Ti:sapphire (800 nm, dashed line) and an infrared laser wavelength (1500 nm, solid line). The double logarithmic plot of the ion yields as a function of intensity shows the typical linear
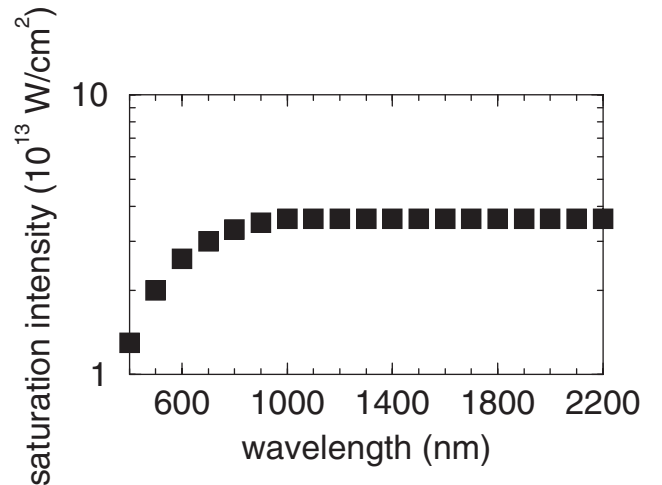

FIG. 2.   Saturation intensities of the first charge state C_{60}^+ as a function of wavelength at a pulse duration of 70 fs.

increase up to saturation. The slope at 800 nm is very similar to that one observed by Tchaplyguine *et al.* [24] as well as to that calculated using the density-functional theory (DFT) by Bauer *et al.* [25]. We note that the presently predicted saturation intensity at 800 nm is closer to the DFT calculation than to the experimental observation. The experimental value, rather unexpectedly, even exceeds the constant value observed in the long wavelength static-field limit [3]. In Fig. 3(b), we have compared the experimentally observed intensity dependence of the ion yields of C_{60}^{3+} and C_{60}^{4+} (open squares, Ref. [15]) at 1500 nm with the corresponding *S*-matrix results (lines). Since the experimental yields are not obtained on an absolute scale, for the sake of comparison, they are required to be matched with the theoretical yields but at one point (with no shift in the intensity scale). We have chosen here a point at the C_{60}^{3+} curve and may emphasize that this alone fixes the scale for the C_{60}^{4+} yields, too. The slopes of the yield curves are seen to agree well with each other; we note an overall but small underestimation of the C_{60}^{4+} data. Before proceeding with the analysis, we may point out that the theoretical predictions are based on sequential single ionization, while nonsequential processes are not considered in the present first-order *S*-matrix theory. The above agreement does therefore confirm earlier conclusions [15] that nonsequential ionization does not play a major role in the ionization of C_{60} to higher charged states.

Finally, we turn to the analysis of the intriguing observation that the saturation intensities of the Buckminster fullerene and its ions are systematically *higher* (and, therefore, the ionization probabilities are lower, at a given intensity) than those of the companion atoms having the same ionization potentials. This behavior is reminiscent of the phenomenon of "suppressed ionization" observed for diatomics [1] and a series of organic molecules [2] in the past. For the diatomics, the phenomenon was interpreted to originate from a molecular "two-slit-like" interference

effect of the ionizing electrons waves emanating from the nuclear centers of the molecule [26]. The experimental data of Bhardwaj *et al.* [3] allow us to investigate a possible similar origin in the case of C_{60} and related icosahedral fullerenes. Thus, we have computed the saturation intensities for the four smallest fullerenes with I_h symmetry, C_{20} ($R \approx 4.0$ a.u.), C_{60} ($R \approx 6.7$ a.u.), C_{80} ($R \approx 7.4$ a.u.), and C_{180} ($R \approx 11.6$ a.u.). The geometrical structures of the fullerenes are obtained using the density-functional tight-binding method [27], which allows for efficient quantum simulations of molecular systems containing several hundreds or thousands of atoms; the ionization potentials are taken from Refs. [28,29]. Indeed, as compared in Fig. 4, we find systematically higher saturation intensities for all the fullerenes (solid circles) than those of the respective hypothetical companion atoms (open squares), calculated using the atomic tunnel model (e.g., [10]). For the companion atom, the ionization potential, the maximum value of the angular momentum, and the number of equivalent electrons have been assumed to be the same as of the HOMO level of the corresponding fullerene (e.g., [30]).

To clarify this further, we note the essential differences between the theoretical models of the fullerenes and the companion atoms. The fullerenes have an extended structure of the nuclear frame which is characterized by a finite cage radius R as well as their many nuclear centers, as opposed to the point nucleus of the companion atoms. First, this seems to affect specifically the degree of the Coulomb correction, given by Eq. (4), since the cage size is large in the former case, but $R = 0$ in the latter case. Second, the presence of the many nuclear centers leads to the "multislit" interference of the partial waves arising from the coherent sum of partial amplitudes in the tran-
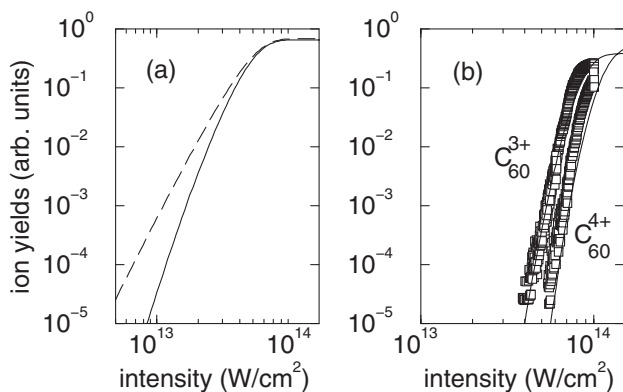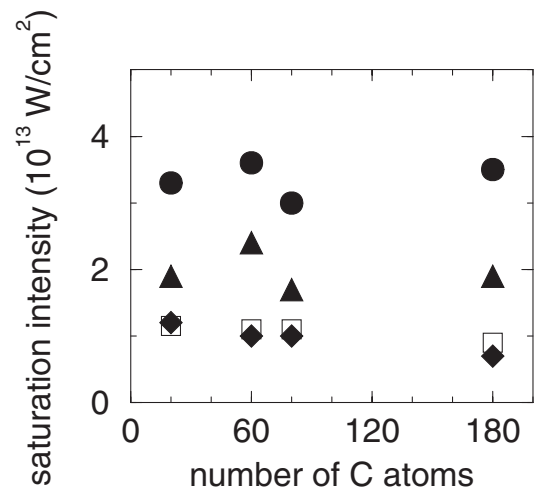

FIG. 3. (a) C_{60}^+ ion yields as a function of peak intensity at 800 nm (dashed line) and 1500 nm (solid line) wavelength. (b) Comparison of the theoretical predictions (lines) for the ion yields of C_{60}^{3+} and C_{60}^{4+} with the experiment data (open squares, [15]) at 1500 nm. Pulse duration: 70 fs.

FIG. 4. Comparison of the saturation intensities for ionization of the four smallest fullerenes C_{20}, C_{60}, C_{80}, and C_{180} having I_h symmetry: full calculations (solid circles), zero-radius approximation (solid triangles), incoherent zero-radius approximation (solid diamonds), and atomic tunneling predictions (open squares). Laser parameters as in Fig. 1.

sition matrix $M_i(\mathbf{k}_N; \mathbf{R}_i)$ in Eq. (2). For the companion atoms, this is obviously absent.

It remains to be investigated whether these two effects indeed lead to the suppression of the ionization probability and give rise to the higher saturation intensities in the case of the fullerenes. To test this explicitly, we have compared the results of the full calculations with those of fictitious model "fullerenes." This is readily accomplished in the present theory by putting the cage radius R in Eq. (4) to zero, as well as replacing the modulo square of the coherent sum of the partial amplitudes M_i in Eq. (2) by the *incoherent* sum of their squares, and repeating the calculations. The saturation intensities obtained for the test cases of the fictitious fullerenes are shown in Fig. 4 as the solid diamonds. They lie invariably below those for the real fullerene counterparts (solid circles) and are very close to those of the companion atoms (open squares). Thus, the above comparison explicitly supports the interpretation that the suppressed ionization of C_{60} and its ions as well as the other icosahedral fullerenes is related to the finite cage size and the multislit interference mechanism. Indeed, both effects contribute significantly to the suppression, as can be seen from the results of test calculations (solid triangles in Fig. 4), where the cage radius in Eq. (4) is set to zero but the coherent sum of the partial amplitudes is retained.

To summarize, we have analyzed using the lowest-order S-matrix theory the saturation intensities of the Buckminster fullerene C_{60} and its ions, as well as of the sequence of the icosahedral fullerenes C_{20}, C_{80}, and C_{180}. It is found that the fullerene molecules exhibit the phenomenon of suppressed ionization; i.e., they are systematically harder to ionize, as measured by the higher saturation intensities, than their companion atoms having the same ionization energy. Excellent agreement between the predictions of the present theory and the recent experimental data for C_{60} and its ions up to C_{60}^{9+} is found. Our analysis strongly suggests that the suppressed ionization of fullerenes is a dynamical one-electron process, dominated by the finite cage size and the multislit destructive interference of electron waves emanating from the many nuclear centers rather than a dynamical multielectron polarization effect.

[1] A. Talebpour, C.-Y. Chien, and S. L. Chin, J. Phys. B **29**, L677 (1996).

[2] S. M. Hankin, D. M. Villeneuve, P. B. Corkum, and D. M. Rayner, Phys. Rev. Lett. **84**, 5082 (2000).

[3] V. R. Bhardwaj, P. B. Corkum, and D. M. Rayner, Phys. Rev. Lett. **91**, 203004 (2003).

[4] K. C. Kulander, Phys. Rev. A **38**, 778 (1988).

[5] B. Walker, B. Sheehy, L. F. DiMauro, P. Agostini, K. J. Schafer, and K. C. Kulander, Phys. Rev. Lett. **73**, 1227 (1994).

[6] R. Shakeshaft, R. M. Potvliege, M. Dörr, and W. E. Cocke, Phys. Rev. A **42**, 1656 (1990).

[7] L. Dimou and F. H. M. Faisal, Phys. Lett. A **171**, 211 (1992).

[8] L. V. Keldysh, Zh. Eksp. Teor. Fiz. **47**, 1945 (1964) [Sov. Phys. JETP **20**, 1307 (1965)].

[9] A. M. Perelomov, S. V. Popov, and M. V. Terent'ev, Zh. Eksp. Teor. Fiz. **50**, 1393 (1966) [Sov. Phys. JETP **23**, 924 (1966)].

[10] M. V. Ammosov, N. B. Delone, and V. P. Krainov, Zh. Eksp. Teor. Fiz. **91**, 2008 (1986) [Sov. Phys. JETP **64**, 1191 (1986)].

[11] X. M. Tong, Z. X. Zhao, and C. D. Lin, Phys. Rev. A **66**, 033402 (2002).

[12] F. H. M. Faisal, J. Phys. B **6**, L89 (1973).

[13] H. R. Reiss, Phys. Rev. A **22**, 1786 (1980).

[14] A. Becker and F. H. M. Faisal, J. Phys. B **38**, R1 (2005).

[15] V. R. Bhardwaj, P. B. Corkum, and D. M. Rajner, Phys. Rev. Lett. **93**, 043001 (2004).

[16] Th. Brabec, M. Coté, P. Boulanger, and L. Ramunno, Phys. Rev. Lett. **95**, 073001 (2005).

[17] Gaussian03, Revision C.02, Gaussian, Inc., Wallingford, CT, 2004 (http://www.gaussian.com).

[18] V. P. Krainov, J. Opt. Soc. Am. B **14**, 425 (1997).

[19] A. Becker, L. Plaja, P. Moreno, M. Nurhuda, and F. H. M. Faisal, Phys. Rev. A **64**, 023408 (2001).

[20] C. Yannouleas and U. Landman, Chem. Phys. Lett. **217**, 175 (1994).

[21] A. Jaroń-Becker, A. Becker, and F. H. M. Faisal, Phys. Rev. A **69**, 023410 (2004).

[22] K. Hoffmann, Ph.D. thesis, Freie Universität, Berlin, 2000.

[23] I. V. Hertel, T. Laarmann, and C. P. Schulz, Adv. At. Mol. Opt. Phys. **50**, 219 (2005).

[24] M. Tchaplyguine, K. Hoffmann, O. Dühr, H. Hohmann, G. Korn, H. Rottke, M. Wittmann, I. V. Hertel, and E. E. B. Campbell, J. Chem. Phys. **112**, 2781 (2000).

[25] D. Bauer, F. Ceccherini, A. Macchi, and F. Cornolti, Phys. Rev. A **64**, 063203 (2001).

[26] J. Muth-Böhm, A. Becker, and F. H. M. Faisal, Phys. Rev. Lett. **85**, 2280 (2000).

[27] D. Porezag, Th. Frauenheim, Th. Köhler, G. Seifert, and R. Kaschner, Phys. Rev. B **51**, 12 947 (1995); G. Seifert, D. Porezag, and Th. Frauenheim, Int. J. Quantum Chem. **58**, 185 (1996); M. Elstner, D. Porezag, G. Jungnickel, J. Elsner, M. Haugk, Th. Frauenheim, S. Suhai, and G. Seifert, Phys. Rev. B **58**, 7260 (1998).

[28] F. A. Gianturco, R. R. Lucchese, and N. Sanna, J. Chem. Phys. **118**, 4013 (2003).

[29] G. Seifert, K. Vietze, and R. Schmidt, J. Phys. B **29**, 5183 (1996).

[30] M. S. Dresselhaus, G. Dresselhaus, and P. C. Eklund, *Science of Fullerenes and Carbon Nanotubes* (Academic, New York, 1996).